

Final Stages of Stellar Evolution
edts. J.-M. Hameury & C. Motch
EAS Publications Series, 2018

EQUATION OF STATE OF DENSE MATTER AND MAXIMUM MASS OF NEUTRON STARS

P. Haensel¹

Abstract. Theoretical models of the equation of state (EOS) of neutron-star matter (starting with the crust and ending at the densest region of the stellar core) are reviewed. Apart from a broad set of baryonic EOSs, strange quark matter, and even more exotic (abnormal and Q-matter) EOSs are considered. Results of calculations of M_{\max} for non-rotating neutron stars and exotic compact stars are reviewed, with particular emphasis on the dependence on the dense-matter EOS. Rapid rotation increases M_{\max} , and this effect is studied for both neutron stars and exotic stars. Theoretical results are then confronted with measurements of masses of neutron stars in binaries, and the consequences of such a confrontation and their possible impact on the theory of dense matter are discussed.

1 Introduction

Since the pioneering paper of Oppenheimer and Volkoff (1939) the problem of the actual value of the maximum mass of neutron stars, M_{\max} , is puzzling both the theorists and observers. Oppenheimer and Volkoff, who used free neutron-gas model, obtained $M_{\max} = 0.72 M_{\odot}$. The precisely known mass of the Hulse-Taylor pulsar is a direct proof of the dominating role of the *nuclear forces* in the equation of state (EOS) of neutron stars, which stiffen the EOS so that $M_{\max} > 1.44 M_{\odot}$. Unfortunately, the value of M_{\max} is determined by the EOS of dense matter at $\rho > 2\rho_0$, where $\rho_0 = 2.7 \times 10^{14} \text{ g cm}^{-3}$ is normal nuclear density, and at such high densities the EOS is largely unknown. This results in a large uncertainty in theoretically derived value of M_{\max} .

Within General Relativity, a compact object of $10 M_{\odot} \gtrsim M > 1 M_{\odot}$ and $R < 50 \text{ km}$ cannot be but a neutron star *or* a black hole. All compact objects with $M > M_{\max}$ are necessarily black holes, while only those with $M < M_{\max}$ can be neutron stars. From the observational point of view, the problem consists

¹ N. Copernicus Astronomical Center, Bartycka 18,
 00-718 Warszawa, Poland, haensel@camk.edu.pl

in determining the *mass function* of neutron stars: its upper edge is just M_{\max} . However, the present measurements of neutron stars masses are most probably strongly biased due to a specific evolutionary formation scenario (binary radio pulsars) or are not very useful due to large errors (X-ray binaries; some possible exceptions are discussed in Sect. 14). Hopefully, the knowledge of neutron-star masses will improve in the future (see discussion in Sect. 14). Then, confrontation of measured masses with theoretical models will give us precious information on the EOS of matter at $\rho \sim 10^{15} \text{ g cm}^{-3}$.

The present paper reviews the status of the theoretical determination of M_{\max} . Sections 2–5 are devoted to a brief description of existing models of the EOS of dense matter. Calculations of neutron-star structure in General Relativity are presented in Sect. 6. In Sects. 6.2–6.3 we discuss the mass–central-density diagram for non-rotating (conventional) neutron stars made of baryons, with particular emphasis on the value of M_{\max} and its dependence on the EOS of baryonic matter, as well as the stability of stellar configurations. Short Sect. 7 is devoted to a discussion of the origin of the maximum of neutron star mass. An upper bound on M_{\max} is studied in Sect. 8. The problem of stability of stellar configurations is reviewed in Sect. 6.3. Phase transitions in dense matter and their impact on neutron-star masses, and in particular on M_{\max} , are described in Sec. 9. Effect of rotation on neutron-star structure and on the maximum mass is discussed in Sects. 10–11. Section 12 is devoted to intriguing (hypothetical) family of strange quark stars, and Sect. 13 – to even more exotic Q-stars. Theoretical values of M_{\max} are confronted with existing measurements of neutron-star masses in Sect. 14. Some final remarks are presented in Sect. 15.

2 Equation of state of the neutron-star crust

We assume that the crust is built of matter in full thermodynamic equilibrium (the so called *cold catalyzed matter* corresponding to minimum energy per nucleon at a given nucleon density); the case of *accreted crust* will be briefly mentioned at the end of the present section. The crust can be divided into an *outer crust*, in which a lattice of nuclei is immersed in an electron gas, and an *inner crust* consisting of a lattice of nuclei immersed in an neutron gas and electron gas. The outer crust ends at the neutron drip point $\sim 4 \times 10^{11} \text{ g cm}^{-3}$, while the inner crust extends down to the crust–core interface at $\sim 10^{14} \text{ g cm}^{-3}$.

Up to the neutron drip point, the EOS can be calculated using the experimental data on the neutron-rich nuclei and semiempirical nuclear mass formulae (Haensel and Pichon 1994). Therefore, the EOS of the outer crust is rather well established. As soon as one leaves the region of experimentally known nuclei, the EOS of cold catalyzed matter becomes uncertain. This uncertainty rises at densities higher than the neutron drip density. The properties of nuclei are affected by the ambient neutron gas which contributes more and more to the total pressure. Therefore, the problem of correct modelling of the EOS of pure neutron gas at subnuclear densities becomes important. The real EOS of cold catalyzed matter stems from the real nucleon Hamiltonian, which is expected to describe nucleon in-

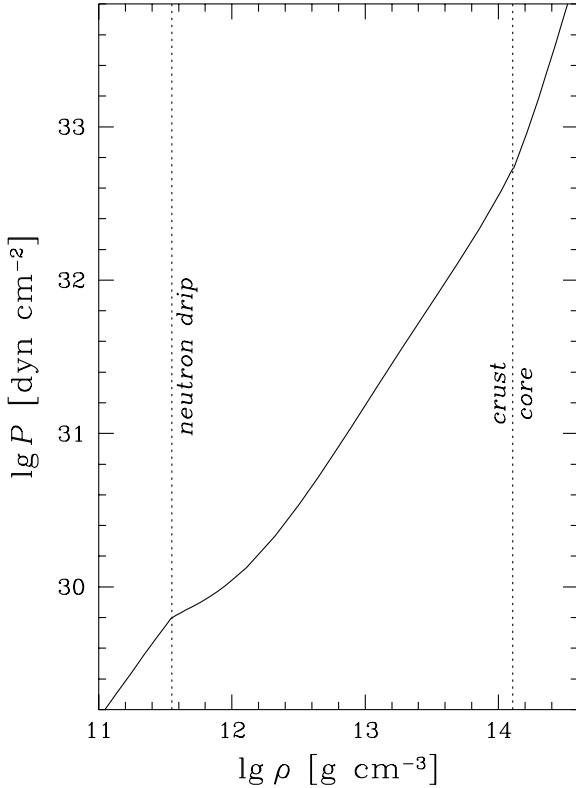


Fig. 1. The SLy EOS (Douchin and Haensel 2001) of neutron star crust. Dotted vertical lines correspond to the neutron drip and crust-core transition.

teractions at $\rho \lesssim 2\rho_0$. In practice, in order to make the solution of the many-body problem feasible, the task is reduced to finding an *effective nucleon Hamiltonian*, which would enable one to calculate reliably the EOS of cold catalyzed matter for $10^{11} \text{ g cm}^{-3} \lesssim \rho \lesssim \rho_0$, including the crust-core transition.

We will illustrate the properties of the inner crust EOS using the results obtained by Douchin and Haensel (2001) for the SLy model of effective nuclear hamiltonian; it will be hereafter referred to as the SLy EOS. Notice that the sound velocity is $v_s = \sqrt{dP/d\rho}$. The overall SLy EOS of the crust, calculated including adjacent segments of the liquid core and the outer crust, is shown in Fig. 1. In the outer crust segment, the SLy EOS cannot be visually distinguished from the EOS of Haensel and Pichon (1994). One notices a significant softening (decrease of v_s) just after the neutron drip point. At densities greater than the neutron drip one, the SLy EOS stiffens gradually (v_s increases) with growing density, due to the increasing contribution of dripped neutrons to the pressure. There

Table 1. Equations of state of the liquid core of neutron star

EOS	composition and model	reference
BPAL12	$npe\mu$, effective nucleon energy functional	Bombaci et al. 1995
BGN1H1	$np\Sigma\Lambda\Xi e\mu$, effective baryon energy functional	Balberg et al. 1999
BBB1	$npe\mu$, Brueckner theory, Argonne NN plus Urbana NNN potentials	Baldo et al. 1997
FPS	$npe\mu$, effective nucleon energy functional	Pandharipande and Ravenhall 1989
BGN2H1	$np\Sigma\Lambda\Xi e\mu$, effective baryon energy functional	Balberg et al. 1999
BBB2	$npe\mu$, Brueckner theory, Paris NN plus Urbana NNN potentials	Baldo et al. 1997
SLy	$npe\mu$, effective nucleon energy functional	Douchin and Haensel 2001
BGN1	$npe\mu$, effective baryon energy functional	Balberg et al. 1999
APR	$npe\mu$, variational theory, Nijmegen NN plus Urbana NNN potentials	Akmal et al. 1998
BGN2	$npe\mu$, effective nucleon energy functional	Balberg et al. 1999

is a discontinuous increase (jump) of sound velocity at the crust-core interface.

In the SLy EOS, the crust-core transition takes place as a very weak first-order phase transition, with the relative density jump of the order of a percent (Douchin and Haensel 2001). Let us remark that for this model the spherical nuclei persist to the crust bottom. For the FPS EOS, the crust-core transition takes place through a sequence of phase transitions with the changes of nuclear shapes (spheres-rods-plates-tubes-bubbles, Lorenz et al. 1993). All in all, while the presence of the exotic nuclear shapes is expected to have dramatic effect on the transport phenomena and elastic properties of matter, their effect on the EOS is small.

Some neutron stars, in particular those in close binary systems, have crust composed of accreted matter. The EOS of *accreted crust* is somewhat stiffer than for the ground-state crust (Haensel and Zdunik 1990). However, the effect of this difference on the value of M_{\max} is negligibly small.

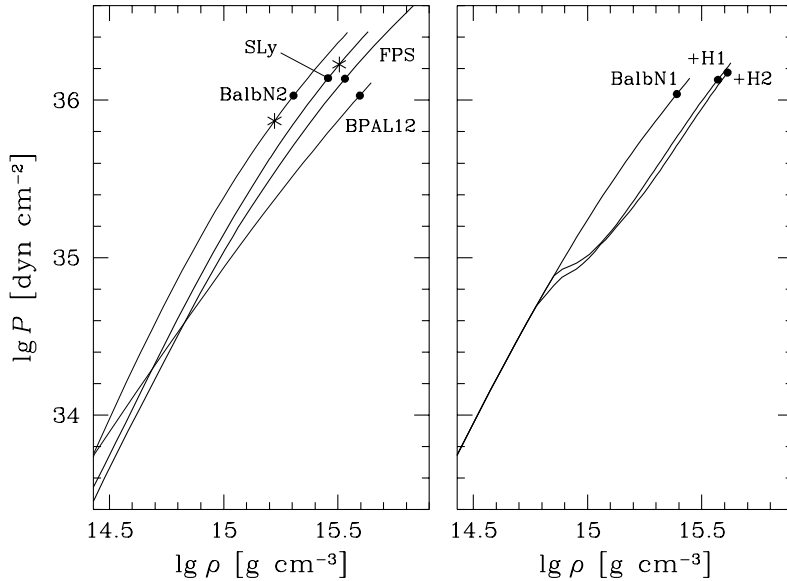


Fig. 2. Selected models of the EOS of neutron star cores denoted as in Table 1, except for the BGN1 and BGN2 which here have labels BalbN1 and BalbN2. Large dots correspond to maximum density in stable neutron stars. Asterisks correspond to the density above which EOS is superluminal ($v_s > c$). Left panel: EOSs of the $npe\mu$ matter. Right panel: effect of hyperons is shown by comparing the EOS without hyperons (i.e., for the $npe\mu$ matter) and EOSs in which hyperons Λ , Σ , Ξ are included (+H1 and +H2 correspond to the BGN1H1 and BGN1H2 models of Table 1).

3 Equation of state of the neutron-star core

At $\rho \lesssim \rho_0$, core matter is a liquid composed mostly of neutrons with a few percent admixture of the equal number of protons and electrons. If the Fermi energy of electrons exceeds the muon rest energy (105.7 MeV), muons replace a fraction of electrons to minimize the energy of the system. Such a system in beta equilibrium is usually called the $npe\mu$ -matter. This is the simplest model of matter in neutron star cores: except for the presence of muons, which are insignificant for the EOS, the matter constituents - neutrons, protons, and electrons - are the same as in familiar terrestrial matter. Still, even for this simplest composition, the uncertainties in the EOS are quite large, especially at densities significantly higher than ρ_0 . This results from the approximations and deficiencies of the many-body theory of dense nucleon matter, and from the lack of knowledge of strong interactions in superdense matter. We illustrate these uncertainties in the left panel of Fig. 2, where four examples of the EOS of the $npe\mu$ -matter are shown. The

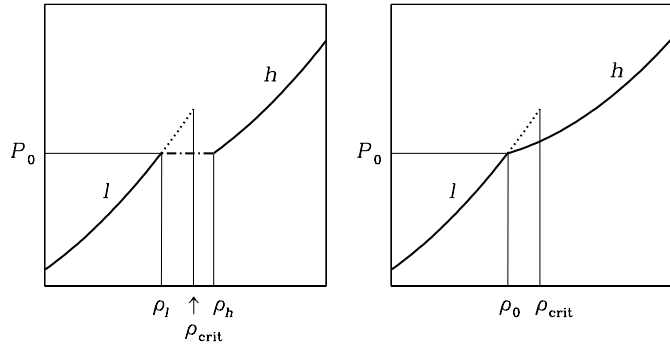


Fig. 3. Effect of phase transitions on the EOS of neutron-star core. Solid line: stable lower-density (l) or higher-density (h) phase. Dotted line: metastable l-phase. The density at which metastable l-phase becomes unstable with respect to the transition into a dense phase is denoted by ρ_{crit} . Left panel: first-order phase transition at $P = P_0$ from a pure l-phase to a pure h-phase, with the density jump at $P = P_0$ from ρ_l to ρ_h . Right panel: transition from l-phase to a mixed h-phase at $P = P_0$ and $\rho = \rho_0$. Notice that here ρ_0 means the threshold density for the equilibrium-phase transition. The right panel could describe also the effect of a second-order phase transition, provided the dotted segment is removed.

brief characteristics of these models and the references to the original papers are given in Table 1. The BPAL12 and BGN2 EOSs should be considered as the soft and stiff extremes of the theoretical models. Only segments below large dots, which correspond to the maximum density in stable neutron stars calculated for this EOS (see Sect. 6.2 and in particular Table 2), are relevant for neutron stars. Notice that the stiffest BGN2 EOS is superluminal (sound velocity $v_s > c$) at the highest densities relevant for neutron stars, which reflects the inadequacy of the non-relativistic approach at such a high density.

Let us denote the chemical potentials of the constituents of the $npe\mu$ -matter by μ_n , μ_p , μ_e , and μ_μ . As soon as the sum $\mu_n + \mu_e$ exceeds the in-medium energy of Σ^- hyperon, this strange baryon will appear in as a stable constituent of dense matter. Σ^- is expected to be the first hyperon to appear in dense matter at some ρ_1 . The second hyperon to appear, above a higher threshold density ρ_2 , is Λ^0 . Hyperons appear due to strangeness-changing weak interactions. At a given baryon density, the inclusion of hyperons lowers significantly the matter pressure compared to the case of the $npe\mu$ matter, because the highest-energy neutrons are then replaced by the low-energy hyperons. This effect of the softening of the EOS of dense matter due to the presence of hyperons is clearly seen in the right panel of Fig. 2.

Pion or kaon condensation in dense matter, as well as deconfinement of quarks, predicted by some theories, imply a softening of the EOS above the phase-transition

threshold. The effect of such a phase transition on the EOS is visualized in Fig. 3.

4 EOS of strange matter

Strange quark matter (SQM) is a hypothetical self-bound state of deconfined quarks which form a plasma of up (u), down (d), and strange (s) quarks with $n_u \simeq n_d \simeq n_s$ of total baryon number density $n_b = (n_u + n_d + n_s)/3$ and a small admixture of electrons $n_e \sim (10^{-5} - 10^{-4})n_b$. The existence of a self-bound state at zero pressure results from the pressure exerted by the ordinary vacuum on a volume of the QCD vacuum in which the quarks can move. In the Bag Model this pressure is equal to the bag constant $B \sim 60 \text{ MeV/fm}^3$. In the simplest Bag Model with massless free quarks the density of SQM at zero pressure is $\rho_s = 4B/c^2$. The hypothesis that SQM is the true ground state of matter at zero pressure means that energy per unit baryon number $E_{\text{SQM}} < E(^{56}\text{Fe}) = 930.4 \text{ MeV}$. Recent reviews of physics of strange quark matter are given by Glendenning (1999), Madsen (1999), and Weber (1999).

As the pressure of SQM vanishes at ρ_s (larger than normal nuclear density ρ_0), the EOS has a linear form $P \simeq (\rho - \rho_s) \times \text{constant}$ for densities only slightly higher than ρ_s . It is very fortunate that this simple linear form of the EOS turns out to be an excellent approximation at higher densities, up to maximum density in stable strange stars. This property is independent of the SQM model, and holds for the MIT Bag Model (Zdunik 2000) and other models of SQM (Gondek-Rosińska et al. 2000).

Let us focus our attention on the Bag Model. A linear approximation reads

$$P/c^2 = a(\rho - \rho_s), \quad (4.1)$$

where *constants* a and ρ_s are determined by fitting the exact EOS (Zdunik 2000). Notice that the linear form, Eq. (4.1), is exact in the case of massless quarks (free or interacting). Using first law of thermodynamics one can easily see that Eq. (4.1) implies

$$n_b(P) = n_s \left[1 + \left(4 - \frac{1}{3a} \right) \frac{P}{\rho_s c^2} \right]^{1/(a+1/3)}, \quad (4.2)$$

where n_s is the baryon density of SQM at zero pressure. Therefore three fitting parameters – ρ_s , n_s , and a – completely determine an EOS of SQM.

5 EOS of abnormal and Q-matter

Several types of hypothetical self-bound state of dense baryon matter, which could constitute true ground state of the matter at $P = 0$, were suggested in the past. In 1970s, it was suggested that the pion condensation could lead to the appearance of a self-bound, superdense state of pion-condensed nucleon matter (Migdal 1971, 1974, Hartle et al. 1975). This phase of matter was expected to form “abnormal nuclei” of large A and with the density significantly higher than ρ_0 (Migdal 1971,

1974) but no sign of experimental evidence of the existence of the “abnormal nuclei” has been found up to the time of this writing.

The idea of “abnormal state” of nuclear matter, as advanced by Lee and Wick (1974; for a review see Lee 1975), is based on a schematic field-theoretical σ -model of strongly interacting nucleon matter. In the abnormal state, which appears at sufficiently high nucleon densities, the nucleons are thought to become nearly massless. This is because the σ -field term couples to the nucleons as an (negative) addition to the nucleon rest (bare) mass, implying a nearly vanishing nucleon effective mass. This density-dependent effect can lead to the appearance of a second minimum in the n_b dependence of the energy per baryon at some n_a , significantly higher than n_0 , with the binding energy significantly larger than in the “normal state” at $n_b = n_0$. However, the original σ -model is schematic and does not pretend to describe quantitatively the normal nuclear matter at $n_b \approx n_0$. Were the σ -model more complicated to give correct quantitative description of the nuclear matter at $n_b \approx n_0$, then the abnormal state at supranuclear density would disappear (Pandharipande and Smith 1975, Moszkowski and Källman 1977).

Supersymmetric extensions of the Standard Model of elementary particles and their interactions predict the existence of macroscopic self-bound superdense lumps of a scalar-field condensate with a well defined electric and baryonic charge – baryonic Q-balls. The Q-balls were proposed as a hypothetical component of cosmological dark matter (Kusenko et al. 1998, Kusenko 2000). It was also proposed that Q-balls of a macroscopic size could have energy per unit baryon number lower than ^{56}Fe . EOSs of Q-matter were constructed by Bahcall et al. (1990). A common feature of these models, shared with the Lee-Wick model of abnormal matter is that nucleons become massless inside the condensed Q-phase. Two basic parameters of the model are: the energy density U_0 of the scalar field inside the Q-matter, and the coupling strength α_v of the vector field to the nucleon. It is convenient to introduce a dimensionless parameter $\zeta = \alpha_v U_0^{1/2} \pi / \sqrt{3}$, and to use it instead of the parameter α_v .

Consider the simplest case of $\zeta = 0$. The standard value used by Bahcall et al. (1990) is $U_0 = 13.0 \text{ MeV fm}^{-3}$, which corresponds to $\rho(P = 0) \equiv \rho_s = 1.0 \times 10^{14} \text{ g cm}^{-3}$: for this model the density of Q-balls is subnuclear. With increasing ζ , the EOS of the Q-matter becomes stiffer and the value of ρ_s lower. In the limiting case of $\zeta = 16$ considered by Bahcall et al. (1990) (at the same value of $U_0 = 13.0 \text{ MeV fm}^{-3}$) they get $\rho_s = 5.5 \times 10^{13} \text{ g cm}^{-3}$. The predicted density of self-bound Q-matter at zero pressure is two to five times lower (!) than the normal nuclear density, which results from a strong reduction of effective nucleon masses in this hypothetical state of nucleon matter.

In all cases considered in the present section, the EOS of an abnormal phase of dense baryonic matter can be well approximated by

$$\text{abnormal matter, Q-matter : } P \simeq a(\rho - \rho_s)c^2. \quad (5.1)$$

This EOS is usually stiffer than that of strange quark matter, and one often has $a \simeq 1$.

Finally, let us stress that there has been no observational evidence for the existence of hypothetical self-bound states of dense matter reviewed in the present section by the time of this writing.

6 Neutron star models

Neutron stars are relativistic objects. Their structure and evolution should be studied using the General Theory of Relativity. The importance of relativistic effects for a star of mass M and radius R is characterized by the *compactness parameter* r_g/R , where $r_g = 2GM/c^2 = 2.95(M/M_\odot)$ km is the gravitational radius. For a non-rotating black hole, $r_g/R = 1$. Typically, one has $r_g/R \sim 0.2 - 0.4$ for a neutron star, while $r_g/R \ll 1$ for all other stars, e.g., $r_g/R \sim 10^{-4}$ for white dwarfs, and $r_g/R \sim 10^{-6}$ for main-sequence stars of $M \simeq 1 M_\odot$.

We will approximate the stress tensor of neutron-star matter by that of a perfect fluid, i.e. non-viscous medium of total energy density \mathcal{E} (mass density $\rho = \mathcal{E}/c^2$), in which all stresses are zero except for an isotropic pressure P . The perfect-fluid approximation is justified by the fact that the shear stresses, e.g., those produced by elastic strain in the solid crust or by strong magnetic field, are generally negligible compared to the pressure.

The problem of finding hydrostatic equilibrium simplifies considerably in the case of strongly degenerate neutron star interior where thermal contributions to P and ρ can be neglected. Then, the EOS of matter involves only P and ρ , but not the temperature, a situation which is nearly always valid in neutron-star interior (important exceptions are: neutron-star atmospheres, newly-born neutron stars, envelopes of exploding X-ray bursters).

For a static spherically symmetric neutron-star configuration the equation of hydrostatic equilibrium is (see, e.g., Shapiro and Teukolsky 1983)

$$\frac{dP}{dr} = -\frac{G\rho m}{r^2} \left(1 + \frac{P}{\rho c^2}\right) \left(1 + \frac{4\pi Pr^3}{mc^2}\right) \left(1 - \frac{2Gm}{c^2r}\right)^{-1}, \quad (6.1)$$

$$\frac{dm}{dr} = 4\pi r^2 \rho, \quad (6.2)$$

where $m(r)$ is the mass contained within a sphere of (coordinate) radius r . Equation (6.2) describes mass balance; its apparently Newtonian form is illusive since the space-time is curved. Equations (6.1)–(6.2) should be supplemented by an EOS, $P = P(\rho)$. The above equations constitute then a closed system of equations to be solved for obtaining $P(r)$, $\rho(r)$ and $m(r)$.

In the stellar interior, $P > 0$ and $dP/dr < 0$. The stellar radius is determined from the condition $P(R) = 0$. Outside the star, i.e., for $r > R$, we have $P = 0$ and $\rho = 0$, and from Eq. (6.2) we obtain $m(r > R) = M = \text{const}$. The latter quantity is called the *total gravitational mass of the star*; the total energy content of a star is $E = Mc^2$.

In order to construct a neutron-star model one has to solve the set of Eqs. (6.1)–(6.2) supplemented by an EOS of neutron-star matter. Let us notice that the mass

density and baryon density are not constrained to be continuous. In principle, density discontinuities can appear at pressures corresponding to first-order phase transitions in dense matter (see Sect. 3). The density profile is determined using the EOS, through $\rho = \rho(P)$.

Equations (6.1)–(6.2) are integrated from the stellar center with the following boundary conditions: $P(0) = P_c$, $m(0) = 0$. The stellar surface, $r = R$, is determined from $P(R) = 0$.

EOS constitutes a crucial input for the neutron-star structure calculations. Models of the EOS were described in Sects. 2–3. Here we briefly describe the EOS used in neutron-star structure calculations discussed in the present paper. The outer neutron-star crust is described by the EOS of Haensel and Pichon (1994). The inner crust is described by the FPS model, developed by Lorenz (1991), except for the SLy EOS, which describes in a unified manner both the core and the crust. Actually, a particular choice of the crustal EOS has little importance for the global parameters of massive neutron-star models, which are mostly determined by the EOS of the liquid core at supranuclear densities.

The EOS of the core is dominated by the contributions from *strong (nuclear) interactions* between nucleons (or, more generally, between baryons; see Sect. 3). The reliability of the theory of a dense, strongly interacting many-body system decreases rapidly with increasing ρ . Moreover, we have very little experimental information about baryonic interactions at supranuclear densities, especially about the interactions involving hyperons which may appear at higher densities. As a consequence, the EOS of neutron-star matter at supranuclear densities is strongly dependent on the specific microscopic theory of dense matter employed.

Our discussion of the impact of the $\text{EOS}(\rho > \rho_0)$ on the neutron-star structure will be based on the limited, but hopefully representative, set of models of dense *baryonic* matter.¹ The selected models of dense cold baryonic matter are listed in Table 1. They were briefly discussed in Sect. 3. As we stressed in Sect. 3, the most important qualitative feature of an EOS at $\rho > \rho_0$ – as far as neutron-star structure is concerned – is its stiffness. A simple definition of the stiffness can be phrased as follows: the higher the value of P at a given ρ , the stiffer the EOS. However, this definition is ambiguous and sometimes misleading. A somewhat better definition relies on the dimensionless adiabatic index $\gamma = (n_b/P)(dP/dn_b)$. However, a core-EOS relevant for the complete family of neutron-star models has to be given for $\rho_0 \lesssim \rho \lesssim (10 - 15)\rho_0$. It can be rather stiff at $\rho \lesssim (2 - 3)\rho_0$, and then become softer at higher ρ , due to the hyperonization of matter with increasing density (see Sect. 3). Therefore, it is useful to base the *effective stiffness* of the EOS on the value of the maximum allowable mass of neutron stars, M_{\max} , which is a functional of the EOS. The topmost EOS in Table 1 is the softest one, and the effective stiffness of the EOSs increases from the top of the table to its bottom

¹Stellar models based on the EOSs including hypothetical exotic phases, such as pion condensate, kaon condensate, and deconfined quark matter, will be considered separately in Sect. 9. A specific case of hypothetical *strange (quark) stars* or even stranger stars built of *abnormal matter* or *Q-matter* will be briefly reviewed in Sect. 12 and 13.

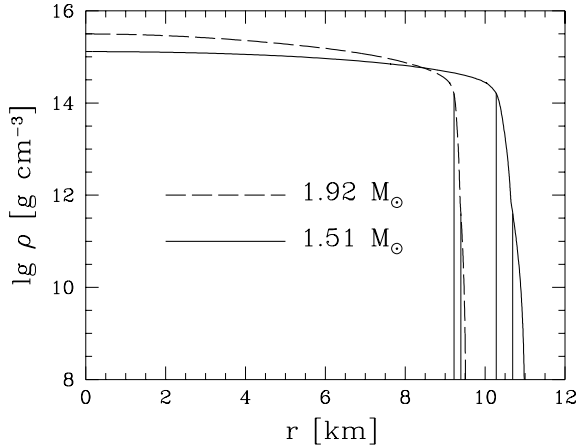


Fig. 4. Mass density versus radial coordinate for neutron-star models of gravitational mass $1.51 M_{\odot}$ (solid line) and $1.92 M_{\odot}$ (long dash-dotted line). Calculations are performed for the BBB2 EOS of the core, for which $1.92 M_{\odot}$ is the maximum allowable mass. The positions of the crust-core interface and the neutron-drip point are indicated by thin vertical lines.

(see Table 2). Let us remind, that the stiffest/softest EOSs are extreme models, characterized by the compression modulus of symmetric nuclear matter, which is significantly higher/lower than the standard “empirical value”. These EOSs are included to represent the theoretical extremes of the EOS of dense matter.

Two of the EOSs listed in Table 1, namely SLy and FPS, are the *unified* ones, and describe, within a single physical model, both the crust and the core of a star (see Sect. 2). In all other cases, an overall EOS of the stellar interior was constructed by matching smoothly the EOS of the crust with that of the core.

6.1 Basic internal structure of neutron stars

The distribution of matter within a neutron star depends on its mass and results from an interplay between the pressure and gravity. In Fig. 4 we show the mass density within a neutron star as a function of radial coordinate, calculated for the BBB2 EOS of the core, for two masses. The higher mass is equal to the maximum mass allowable for this EOS. The calculations show that the density within the core is rather uniform, for $M = (1.2 - 1.5) M_{\odot}$; the most pronounced drop occurs close to the crust bottom edge. There is a steepening of the density drop near the

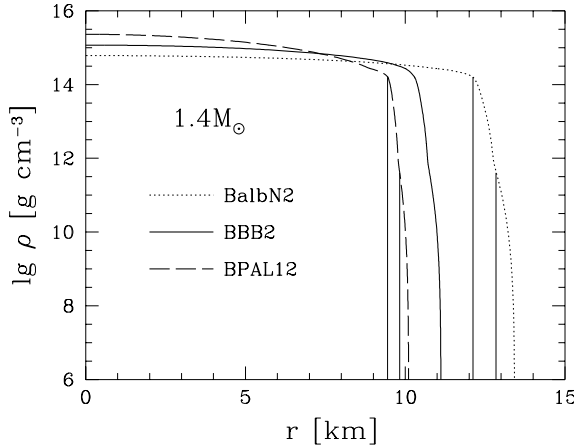


Fig. 5. Mass density versus radial coordinate for neutron-star models of gravitational mass $1.4 M_\odot$, for the core described by the BPAL12 EOS (long dash-dotted line), BBB2 EOS (solid line), and BalbN2 (denoted as BGN2 in Table 1) EOS (dotted line). For the BPAL12 and BalbN2 models, positions of the crust-core interface and the neutron-drip point are indicated by thin vertical lines.

neutron drip point, which results from the softening of the EOS due to the neutron drip. The increase of the stellar mass increases the gravitational pull within the crust, which leads to the steepening of density profiles and thinning of the crust, most pronounced at $M = M_{\max}$. For a medium-stiff BBB2 EOS of the core, the crust contains 1.4% and 0.8% of the total gravitational mass of $1.24 M_\odot$ and $1.51 M_\odot$ stars, and the crust thickness is 1.01 km and 0.72 km, respectively. At the maximum mass, the crust contains only 0.2% of the stellar mass, and the crust thickness reduces to about 0.29 km. The crust mass and thickness are smaller for softer EOSs of the core, and larger for stiffer ones.

While the crustal EOS is rather well established (see Sect. 2), the crust structure results from the interplay of its EOS and the gravitational pull exerted by the core: the latter depends on the core compactness. Therefore, the uncertainty of the EOS in the core implies uncertainty in the crust structure. This is visualized in Fig. 5, where we show the mass density profiles inside a $1.4 M_\odot$ star calculated for the BPAL12, BBB2, and BGN2 EOSs of the core. The crust thickness ranges from 0.7 km for the softest core EOS up to 1.3 km for the stiffest one. The dependence of the fraction of stellar mass contained in the crust on the core EOS is even more

Table 2. Maximum mass configurations for EOSs listed in Table 1. Displayed parameters are: radius R , compactness parameter r_g/R , central baryon density n_c , and central mass density ρ_c .

EOS	M_{\max} [M_\odot]	R [km]	r_g/R	n_c [fm $^{-3}$]	ρ_c [10 15 g cm $^{-3}$]
BPAL12	1.46	9.00	0.480	1.76	3.94
BGN1H1	1.64	9.38	0.519	1.60	3.72
BBB1	1.79	9.66	0.547	1.37	3.09
FPS	1.80	9.27	0.572	1.46	3.40
BGN2H1	1.82	9.53	0.564	1.45	3.48
BBB2	1.92	9.49	0.596	1.35	3.20
SLy	2.05	9.99	0.605	1.21	2.86
BGN1	2.18	10.9	0.592	1.05	2.26
APR	2.21	10.0	0.651	1.15	2.73
BGN2	2.48	11.7	0.626	0.86	2.02

dramatic: this fraction ranges from 0.7% for the softest BPAL12 EOS to 2.2% for the stiffest BGN2 one. The BBB2 model is typical for medium-stiff EOSs: the crust thickness is about 0.8 km and the mass fraction is 1%, respectively.

6.2 Mass–central-density diagram and M_{\max}

The models of cold, static neutron stars form a one-parameter family; they can be labelled by their central density ρ_c , or central pressure P_c . In Fig. 6 we show dependence of the gravitational mass, M , on ρ_c for some EOSs from Table 1 at $\rho_c > 2.5 \times 10^{14}$ g/cm 3 .

On the lower-density side, the $M(\rho_c)$ curves exhibit a minimum $M_{\min} \simeq 0.1 M_\odot$, which depends rather weakly on the assumed EOS (Haensel et al. 2001), and which is not shown in Fig. 6.

On the higher-density side, the $M(\rho_c)$ curves exhibit a maximum, which strongly depends on the assumed EOS, and is reached at densities a few times 10 15 g cm $^{-3}$. Configurations with $M > M_{\max}$ cannot exist in hydrostatic equilibrium and must necessarily collapse into black holes. For the selected EOSs M_{\max} ranges from 1.46 M_\odot to 2.48 M_\odot (Table 2).

Replacing neutron-star matter by a free (noninteracting) Fermi gas of neutrons lowers the value of M_{\max} to 0.72 M_\odot (Oppenheimer and Volkoff 1939). If one further allows for the beta equilibrium between otherwise noninteracting nucleons, electrons, and muons, the EOS becomes even softer, with $M_{\max} = 0.70 M_\odot$. Clearly, the values of M_{\max} obtained neglecting nuclear interactions are in contradiction with precisely measured masses of the binary radio pulsars (Sect. 14). Turning the argument around, we may say that the measured mass 1.44 M_\odot of

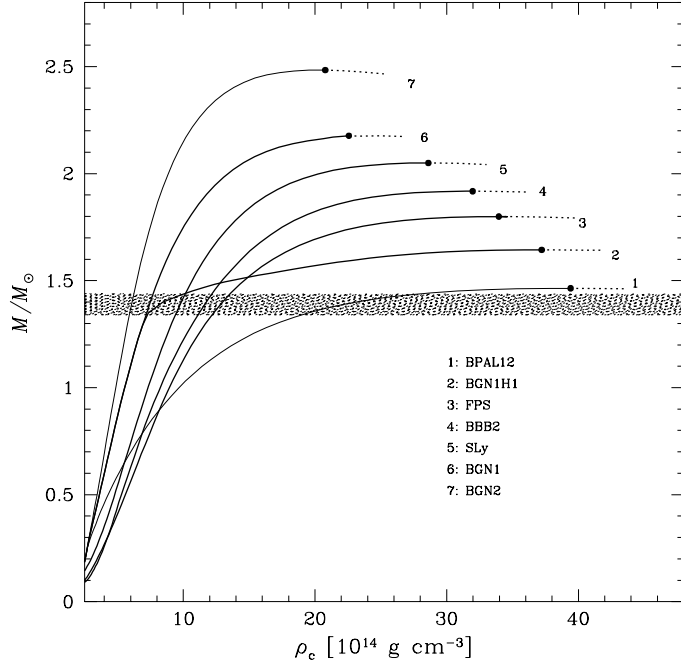


Fig. 6. Gravitational mass M versus central density ρ_c of static neutron-star models for different EOSs. A maximum on a $M - \rho_c$ curve is indicated by a filled circle. Configurations to the right of the maximum are unstable with respect to small radial perturbations, and are denoted by dotted lines. The shaded band corresponds to the range of precisely measured masses of binary radio pulsars (Sect. 14).

the Hulse-Taylor pulsar (Sect. 14) implies that nucleon-nucleon interaction is sufficiently repulsive at supranuclear densities to lift M_{\max} by more than hundred percent from the non-interacting nucleon gas value.

In view of uncertainties in the hyperon-nucleon (H-N) and hyperon-hyperon (H-H) interaction in dense matter, let us first consider a subset of EOSs with $N\mu$ composition of matter (N denotes np). Let us remove from this subset the extreme models BPAL12 and BGN2. Then the subset will be restricted to the models of the $N\mu$ matter which reproduce empirical saturation properties of nuclear matter (see Sect. 3). Under such conditions, we narrow the range of theoretical maximum allowable mass of neutron stars,

$$M_{\max}(N\mu) \simeq (1.8 - 2.2) M_{\odot} . \quad (6.3)$$

The appearance of hyperons softens an EOS, and therefore decreases the value of

M_{\max} . For the selected EOSs, the appearance of hyperons at $\rho \simeq 2\rho_0$ lowers the value of maximum allowable mass to an even narrower range,

$$M_{\max}(\text{NHe}\mu) \simeq (1.5 - 1.8) M_{\odot} . \quad (6.4)$$

Let us stress that this conclusion is obtained under the assumption that the hyperons appear at about $2\rho_0$. However, the threshold for the hyperon appearance depends sensitively on the N-H interaction in dense matter, which is poorly known for a neutron rich dense matter at $\rho \gtrsim \rho_0$. Therefore, the values of M_{\max} in Eq. (6.4) have to be taken with a grain of salt. Actually, it is reasonable to say that Eq. (6.4) corresponds to a typical effect of hyperons on M_{\max} (and on neutron-star structure), assuming that without hyperons M_{\max} is given by Eq. (6.3). Alas, the lack of knowledge of the H-H interaction implies large uncertainty in the effect of hyperons on M_{\max} . For example, an EOS calculated by Vidaña et al. (2001) shows particularly strong softening due to the hyperonic interactions, with $M_{\max}(\text{Ne}\mu) = 1.89 M_{\odot}$ and $M_{\max}(\text{NHe}\mu) = 1.34 M_{\odot}$. The last value contradicts the measured mass of the Hulse-Taylor pulsar. When Vidaña et al. (2001) remove (artificially) the H-H interaction they get $M_{\max}(\text{NHe}\mu) = 1.47 M_{\odot}$, which is marginally acceptable.

6.3 Stability of neutron stars

The mass-central density diagram shows that cold, static equilibrium configurations of neutron stars can exist only for $M_{\min} < M < M_{\max}$. The value of M_{\min} seems to be rather well established, $M_{\min} \simeq 0.1 M_{\odot}$ (see Haensel et al. 2002 and references therein). Equilibrium configurations of neutron stars with $M < M_{\min}$ do not exist.

Non-rotating configurations with $M > M_{\max}$ collapse into black holes. Numerical simulations of such a collapse were performed by several authors, e.g., by Gourgoulhon and Haensel (1993) and Baumgarte et al. (1996a,b).

While all points on the $M(\rho_c)$ curve in Fig. 6 correspond to the configurations of hydrostatic equilibrium, only the points which correspond to *stable equilibrium* are of astrophysical interest. At a given total baryon number, hydrostatic equilibrium corresponds to the extremum of M which is a functional of matter density distribution ρ ; this is equivalent to the vanishing of the first-order variation of M , due to perturbation of ρ denoted as $\delta\rho$. However, this does not guarantee that the second-order variation, quadratic in $\delta\rho$, is positive, which is necessary for the hydrostatic stability. It can be shown (Harrison et al. 1965, Zeldovich and Novikov 1971) that stable equilibria correspond to the segments of the $M(\rho_c)$ curve for which $dM/d\rho_c > 0$; this is the *static stability criterion*. Therefore, the configurations to the right of the maxima in Fig. 6 are unstable with respect to small radial perturbations.² In view of this, $\rho_{c,\max}$ is the maximum density which

²Actual perturbations of neutron stars are time-dependent, and can be decomposed into normal pulsation modes. Assuming that pulsations do not move neutron-star matter from its

can be reached in the interior of stable static neutron stars. The value of the limiting density $\rho_{c,\max}$ in static, cold neutron stars is even more uncertain than the value of M_{\max} : it ranges from $2 \times 10^{15} \text{ g cm}^{-3}$ (about $7\rho_0$) for the stiffest EOS to $4 \times 10^{15} \text{ g cm}^{-3}$ (about $15\rho_0$) for the softest one. It should be stressed that even $7\rho_0$ is very far beyond the limits within which our models of dense neutron star matter can be considered as reliable and unambiguous.

7 On the origin of M_{\max}

When explaining the very existence of M_{\max} , two kinds of general physical arguments can be used. They are associated with expected behavior of cold matter at ultrahigh densities and with General Relativity.

The arguments based on the high-density behavior of the EOS of dense matter were proposed, for Newtonian stars, by Landau (1932). His brief paper presented a general physical argument why above some M_{\max} a large self-gravitating sphere of cold matter cannot sustain itself against gravitational collapse.³ Harrison et al. (1965) rephrased the arguments in a way applicable to neutron stars. However, it should be stressed that this way of reasoning is based on the assumption that in the high-density region in which the stability is lost the EOS of dense matter is that of the ultra-relativistic free Fermi gas. The counterexample to such a behaviour was presented by Zeldovich (1962).

Irrespectively of the form of the EOS of dense matter, the upper bound on M is a consequence of the General Relativity. Consider the right-hand-side of the OV equation of hydrostatic equilibrium, Eq. (6.1). It describes gravitational pull acting on a unit proper-volume of matter,

$$\text{gravitational pull} = -\frac{Gm\rho}{r^2} \left(1 + \frac{4\pi P}{mr^3}\right) \left(1 + \frac{P}{\rho c^2}\right) \left(1 - \frac{2Gm}{rc^2}\right)^{-1}. \quad (7.1)$$

The gravitational pull is given by a Newtonian-like term $-Gm\rho/r^2$, multiplied by three relativistic factors. With increasing M , all three factors in brackets amplify the pull compared to the Newtonian case, and the increase of M with an increase of central pressure P_c becomes harder. Mathematically, the derivative dM/dP_c decreases with growing M .

Let us illustrate this property with an *unphysical* case of incompressible fluid of mass density $\rho_{\text{inc}} = \text{constant}$. The total gravitational mass is then $(4\pi/3)\rho_{\text{inc}}R^3$, and the pressure profile within the star is determined analytically (solution was obtained by Karl Schwarzschild in 1916, and is described in Box 23.2 of Misner et

ground state (i.e., that the EOS for both static and pulsating configurations is the same) one can show that the configurations to the right of M_{\max} in Fig. 6 are indeed unstable with respect to the fundamental mode of small radial pulsations (Harrison et al. 1966). The finite timescale of reactions between constituents of neutron star matter which may be longer than the pulsation period complicates the *dynamical* analysis of stability of neutron stars with respect to small radial pulsations (Meltzner & Thorne 1967, Chanmugan 1976, Gourgoulhon et al. 1995).

³Landau's paper was submitted for publication before discovery of neutron.

al. 1973). The central pressure P_c can be determined as a function of r_g/R . As the mass increases, P_c as well as r_g/R increase monotonically, too. For $P_c \rightarrow \infty$, the radius tends to a finite value $R_{M_{\max}} = \frac{9}{8}r_g$, and therefore the mass tends to

$$M_{\max}^{(\text{inc})} = \frac{4\pi}{9} \frac{R_{M_{\max}} c^2}{G} = \frac{4c^3}{3^{5/2} \pi^{1/2} G^{3/2} \rho_{\text{inc}}^{1/2}} = 5.09 \text{ M}_\odot \left(\frac{5 \times 10^{14} \text{ g cm}^{-3}}{\rho_{\text{inc}}} \right)^{\frac{1}{2}} \quad (7.2)$$

This limit is the General Relativity effect: there is no limit to the mass of the incompressible-fluid stars in Newtonian gravitation. If M_{\max} exists for an incompressible fluid, then *a fortiori* it should exist for *any* EOS of dense matter with finite compressibility. However, the numerical value of M_{\max} is mainly determined by the EOS for $\rho \gtrsim 2\rho_0$ which is largely unknown.

8 Upper bound on M_{\max}

In view of the uncertainty in the value of M_{\max} , it is of interest to have a possibly firm upper bound on M_{\max} . Let us assume that the EOS is known up to a certain density ρ_m . This reliably known segment of the EOS will be denoted by $P_<(\rho)$. It spans the range $0 < P \leq P_u \equiv P_<(\rho_u)$. Having fixed $P_<(\rho)$, we can treat M_{\max} as a *functional* of the EOS at $P > P_u$; this *unknown* EOS will be denoted as $P_>(\rho)$. The inverse function $\rho_>(P)$, determined for $P > P_u$, does not need to be continuous. Let us require only that the $P_>(\rho)$ is subluminal and fulfills the condition of stability:

$$0 < v_s^2 = \frac{dP_>}{d\rho} \leq c^2, \quad (8.1)$$

where v_s is the speed of sound in the dense medium. Our task is to find the maximum of the functional $M_{\max}[P_>(\rho)]$ on a set $\{P_>(\rho)\}$ of EOSs which satisfy conditions (8.1). As it turns out, M_{\max} is maximized by the so called *causal-limit (CL) EOS*,

$$P_>^{\text{CL}}(\rho) = P_u + (\rho - \rho_u)c^2, \quad (8.2)$$

which therefore yields the upper bound we are looking for, M_{\max}^{CL} . It is quite natural: the CL EOS is the stiffest one at $\rho > \rho_u$. Numerical calculations show that for $\rho_u \lesssim 2\rho_0$ the effect of the outer layers with $\rho < \rho_u$ on the value of M_{\max}^{CL} is negligibly small. Actually, had we used the *pure causal-limit EOS* of the form $P = (\rho - \rho_s)c^2$ (where ρ_s is the surface density of a star built of matter with such an EOS), we would slightly increase (by less than one percent) the value of M_{\max} compared to that obtained for the CL EOS with $\rho_u = \rho_s$.⁴ This can be easily explained, because $P_<(\rho)$ is not maximally stiff. All in all, for $\rho_u \lesssim 2\rho_0$ one gets (Rhoades and Ruffini 1974, Hartle 1978, Kalogera and Baym 1996, Glendenning

⁴For a pure CL EOS one gets an exact result $M_{\max} = 3.0 (5 \times 10^{14} \text{ g cm}^{-3}/\rho_s)^{1/2} \text{ M}_\odot$.

1999)

$$v_s \leq c \implies M_{\max} \leq M_{\max}^{\text{CL}} = 3.0 \left(\frac{5 \times 10^{14} \text{ g cm}^{-3}}{\rho_u} \right)^{\frac{1}{2}} M_{\odot}. \quad (8.3)$$

The maximum allowable mass for any EOS($\rho > \rho_u$) with subluminal sound velocity is lower than the above upper bound. As the inequality (8.3) is widely accepted, it seems to be safe to say that actual M_{\max} of static neutron stars built of baryonic matter is below $3 M_{\odot}$.⁵ A rapid rotation increases the value of M_{\max}^{CL} , as discussed in Sect. 11.

9 Phase transitions in dense matter, third family of compact stars, and maximum mass

The existence of exotic phases of dense matter in neutron star cores is a subject of debate. Unfortunately, since the physics of dense matter at $\rho \gtrsim 2\rho_0$ is uncertain, the problem cannot be solved within the present many-body theory. Therefore one is forced to admit that the question: *is a specific exotic phase of dense matter present in a neutron star core?* can only be answered by unambiguous identification of signatures of this phase in neutron star observations.

In what follows, we will distinguish the case of a moderate and a strong softening of an EOS by a phase transition. We will refer to a phase transition as *moderate*, if it does not lead to the appearance of an unstable segment in the $M - \rho_c$ curve. In the opposite case of a *strong softening* of the EOS, the phase transition will imply the existence of an unstable segment of the $M - \rho_c$ curve, which will separate a family of lower-density configurations from a distinct family of superdense compact objects. Let us start with the case of the moderate softening of the EOS, without density jump (right panel of Fig. 3). Then $\rho(P)$ is continuous, $\lambda \equiv \rho_h/\rho_l = 1$, but the adiabatic index $\gamma = (n_b/P)dP/dn_b$ suffers a jump (a drop) at the appearance of a new phase at $P = P_0$. The $M - \rho_c$ curve is displayed in Fig. 7a. Such a situation corresponds to hyperonization, and also to transitions to a mixed phase (baryons and pion or kaon condensate, baryons and deconfined quark matter). In the latter case, the mixed phase exists up to some limiting density at which a transition from a mixed phase to a pure higher-density phase takes place; it is accompanied by a second discontinuous change (actually, an increase) in γ .

Consider now a phase transition which implies a strong softening of the EOS without a density jump. This is the extreme case of a very strong decrease of γ after the phase transition discussed above, followed by a hardening of the EOS at still higher densities. In this extreme situation the $M - \rho_c$ curve has two stable

⁵Notice that we assume that neutron star has an outer layer of density $\rho < \rho_u$, composed of normal cold dense matter. For some very exotic hypothetical models of compact stars with superdense surface built, e.g., of a self-bound Q-matter, the limit of $3 M_{\odot}$ does not apply (Sect. 13).

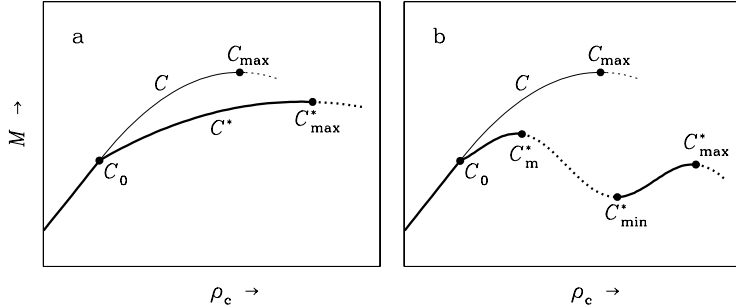


Fig. 7. Mass – central-density relations for an EOS, for which a phase transition at a pressure P_0 implies softening with no density jump (right panel of Fig. 3). Configuration C_0 is the last one composed exclusively of a lower-density phase, its central pressure $P_c = P_0$. Thin lines represent configurations calculated using the EOS without a phase transition. Thick lines show configurations calculated for the EOS with a phase transition. Dotted segments correspond to configurations which are unstable with respect to small radial perturbations. Left panel (a): moderate softening of the EOS. Right panel (b): strong softening of the EOS, implying appearance of an unstable branch between C_m^* and C_{\min}^* (thick dotted line), and a *separate branch of superdense stars* between C_{\min}^* and C_{\max}^* .

branches of static equilibrium configurations, Fig. 7b, corresponding to two distinct families of neutron stars. The first (lower-density or normal) family is continuously connected with low-mass neutron stars and terminates at C_m^* . The second family contains “compact neutron stars”, and will be referred to as the “higher-density family” or “superdense family”. The configurations belonging to the superdense family have central densities $\rho_{\min}^* < \rho_c^* < \rho_{\max}^*$ and masses $M_{\min}^* < M^* < M_{\max}^*$. They are more compact and tightly bound than those containing the same number of baryons and belonging to the normal branch.

The appearance of a distinct family of superdense stars deserves a general remark. Superdense stars form actually the *third family of compact stars* built of degenerate matter, the remaining two being the well known white dwarfs and “lower-density” neutron stars.

Two examples of the strong softening of the EOS without density jumps are given by Glendenning and Kettner (2000) and Schaeffner-Bielich et al. (2002). In the model of Glendenning and Kettner (2000) the softening of the EOS results from the appearance of a quark-baryon mixed phase and takes place for a substantial quark fraction. At higher densities, their EOS stiffens when the mixed phase is replaced by a pure quark phase. In the model of Schaeffner-Bielich et al. (2000) the softening is due to a copious appearance of hyperons. It is obtained for a specific model of hyperon-hyperon interaction. It is followed by a substantial stiffening of the EOS at higher densities. Similarly to the first example, it leads to

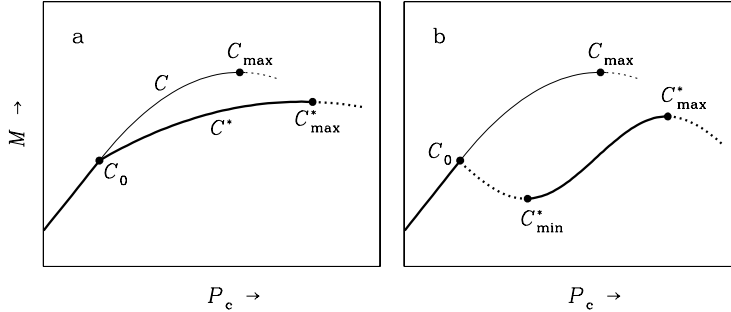


Fig. 8. Mass – central-pressure relations for an EOS containing a phase transition with a density jump (left panel of Fig. 3). Configuration C_0 is the last one composed exclusively of a lower-density phase, with $P_c = P_0$. Notations are the same as in Fig. 7. Panel (a): moderate softening of the EOS. Panel (b): strong softening of the EOS, implying appearance of an unstable branch between C_0 and C_{\min}^* (thick dotted line), and a separate branch of *superdense stars* between C_{\min}^* and C_{\max}^* . For further explanation see the text.

the appearance of the second stable “higher-density branch” of the $M - \rho_c$ curve; the models belonging to this branch are mostly composed of hyperons. In both examples, the maximum mass of the “higher-density branch” is lower than that of the “lower-density” family, $M_{\max}^* < M_{\max}$.

At the same baryon number, the energy M^*c^2 of the high-density configuration is lower. Let A_{\min}^* and A_{\max}^* denote the limiting baryon numbers of stable configurations on the higher-density branch. Configurations with extremal mass and extremal baryon number coincide (see, e.g., Harrison et al. 1965). For $A_{\min}^* < A < A_{\max}^*$, the true stable configurations are those belonging to the higher density branch, while the configurations consisting of the same number of baryons and lying on the lower-density branch are *metastable*.

As a third type of phase transition in dense matter, we consider a transition with a moderate softening associated with a density jump in the EOS. This jump occurs at a pressure P_0 , at which a pure lower-density l-phase of density ρ_l coexists with a pure higher-density **h-phase** of density ρ_h , so that the relative density jump is $\lambda = \rho_h/\rho_l > 1$ (left panel of Fig. 3). In view of the discontinuity of ρ_c at P_0 , the equilibrium configurations have to be parametrized by the central pressure P_c .

One has to stress a particular role played by the quantity

$$\lambda_{\text{crit}} \equiv \frac{3}{2} \left(1 + \frac{P_0}{\rho_l c^2} \right). \quad (9.1)$$

A moderate softening associated with a first order phase transition corresponds to $\lambda < \lambda_{\text{crit}}$.

Finally, we will consider the strong softening of the EOS associated with a first order phase transition with $\lambda = \rho_h/\rho_l > \lambda_{\text{crit}}$. In this case, the appearance

of a small core of h-phase destabilizes the neutron star. Specifically, for static configurations \mathcal{C}^* with a small h-core and $\lambda > \lambda_{\text{crit}}$ one has $dM/d\rho_c < 0$. Such configurations are therefore *unstable* with respect to small radial perturbations and collapse into *stable* configurations with a large h-core. The *instability condition* $\lambda > \frac{3}{2}(1 + P_0/\rho_1 c^2)$ was first derived by Seidov (1971), using the static energy method. Ten years later this condition was rediscovered by Kaempfer (1981) who studied the necessary condition for the onset of the neutron-star collapse initiated by the phase transition at its center. It is worth to mention that the Newtonian version of this criterion ($\lambda > \frac{3}{2}$) was first derived by Lighthill (1950, see also Ramsey 1950) in the context of stability of two-phase planets. The relativistic effects stabilize neutron stars with small h-cores by $\Delta\lambda_{\text{crit}} = \lambda_{\text{crit}} - \frac{3}{2} = \frac{3}{2}P_0/\rho_1 c^2$, which can be as high as ~ 0.2 . Static stable equilibrium configurations of neutron stars split into two families, visualized in Fig. 8b. The superdense branch $\mathcal{C}_{\text{min}}^* \mathcal{C}_{\text{max}}^*$ forms a *third family of compact stars*, apart from the white dwarfs and lower-density neutron stars. It should be stressed, that in contrast to the instability implied by a second-order phase transition due to the hyperonization or appearance of a mixed quark-baryon phase (Sect. 3), a typical situation for $\lambda > \lambda_{\text{crit}}$ corresponds to $M_{\text{max}} < M_{\text{max}}^*$ and $A_{\text{max}} < A_{\text{max}}^*$ (see, e.g., Brown and Weise 1976, Haensel and Prószynski 1982, and Migdal et al. 1990).

10 Rotating neutron stars

We limit ourselves to a stationary rigid rotation. In this case the angular frequency Ω of rotation of a matter element, measured by an observer at infinity, is constant. A rotating configuration has axial symmetry with respect to the rotation axis. A stationary rotation of stellar bodies in General Relativity has been studied by many authors; the present state of this field is reviewed in a *Living Review* by Stergioulas (2001).

Rotating configurations form a two-parameter family, and can be labeled, e.g., by the values of ρ_c and Ω . These configurations are flattened and their equatorial radius, R_{eq} , is larger than the polar radius, R_{pol} . Configurations $\mathcal{C}(\rho_c, \Omega)$ cover a region in the $M - R_{\text{eq}}$ plane. A curve $M(R_{\text{eq}}, \Omega)$ for a fixed Ω is limited on the high- and low-density sides. On the high-density side, the curves are limited by the condition of stability with respect to small axi-symmetric perturbations. In order to check whether a configuration $\mathcal{C}(\rho_{c1}, \Omega_1)$ with angular momentum J_1 is stable, one has to consider a family of configurations $\mathcal{C}(\rho_c, J_1)$ with fixed angular momentum $J = J_1$ in the neighborhood of $\mathcal{C}(\rho_{c1}, \Omega_1)$. Configuration $\mathcal{C}(\rho_{c1}, \Omega_1)$ is stable if

$$\left[\left(\frac{\partial M}{\partial \rho_c} \right)_{J=J_1} \right]_{\rho_c=\rho_{c1}} > 0 , \quad (10.1)$$

where the derivative is calculated along the $\{\mathcal{C}(\rho_c, J_1)\}$ family. A line determined by $(\partial M/\partial \rho_c)_J = 0$ separates the configurations stable with respect to small ax-

isymmetric perturbations from the unstable ones.⁶

The low-density boundary is determined by the condition of stability with respect to the mass-shedding from the equator. A necessary condition for the existence of a stationary rotating configuration is the following: the equatorial velocity of an element of stellar matter has to be smaller than the velocity of a test particle moving on a circular orbit of radius R_{eq} in the equatorial plane, the so-called Keplerian velocity U_K . The Keplerian velocity corresponds to the *Keplerian angular frequency* $\Omega_K = U_K/R_{\text{eq}}$, called also the *mass-shedding angular frequency*.

In order to illustrate the effect of rotation on the structure of *observed pulsars*, consider the radio pulsar PSR B1937+21 with shortest observed period effect of rotation $P_{\text{min}}^{\text{obs}} = 1.56$ ms (Backer et al. 1982); the corresponding angular frequency is $\Omega_{\text{max}}^{\text{obs}} = 641$ Hz. The effect of rotation on the maximum-mass configuration is very small. For $M \simeq M_{\text{max}}$ the period of 1.56 ms corresponds to the *slow rotation regime* ($\Omega \ll \Omega_K$), and therefore $M_{\text{max}}^{1.56\text{ms}} - M_{\text{max}}^{\text{stat}}$ is quadratic in the small parameter $\bar{\Omega} = \Omega/\sqrt{GM/R^3}$. Consider for example the specific case of the SLy EOS (Douchin and Haensel 2001). Then $\bar{\Omega}^2 = (\bar{\Omega}_{\text{max}}^{\text{obs}})^2 \simeq 0.06$. As will be shown in Sect. 11, the highest rotation frequency allowed by the condition of stationarity implies the increase of M_{max} by some 20%. Therefore, the fractional increase of M_{max} connected with rotation at $P = 1.56$ ms is $0.2(\bar{\Omega}_{\text{max}}^{\text{obs}})^2 \simeq 2\%$, which agrees very well with the exact numerical result (Haensel & Douchin 2001). The effect will be smaller for a softer EOS (e.g., FPS EOS) and larger for a stiffer EOS (e.g., APR EOS).

11 Maximum mass of rotating neutron stars

Rotation increases M_{max} because the centrifugal forces oppose the gravity. For $\Omega \ll \Omega_K$, this increase is quadratic in Ω/Ω_K and therefore very small. More generally, $M_{\text{max}}(\Omega) - M_{\text{max}}^{\text{stat}}$ is an even function of Ω , because it does not depend on the orientation of the spin axis.⁷

Within the entire set of stable stationary configurations $\{\mathcal{C}(\rho_c, \Omega)\}$ one can find two important extremal configurations: with the maximum mass $M_{\text{max}}^{\text{rot}}$ and with the minimum period P_{min} . These two configurations do not coincide but are very close to each other. Depending on the EOS, the *maximally rotating configuration* with the rotation period P_{min} can have the central density higher or lower than the maximum-mass configuration, but the difference is at most a few percent (Cook et al. 1994). As a rule, the mass of the maximally rotating configuration is lower than $M_{\text{max}}^{\text{rot}}$ by less than one percent (Cook et al. 1994).

⁶In the static limit, $J_1 = 0$, we recover the condition of stability with respect to radial perturbations (which are a special case of axisymmetric perturbations), $dM/d\rho_c > 0$ (see Sect. 6.3).

⁷We remind that our stars are built of an ideal fluid and the effects of the magnetic fields are neglected.

It is useful to note that for realistic baryonic, subluminal ($v_s \leq c$) EOSs, M_{\max}^{rot} is (to a very good approximation, typically within 3%) proportional to the maximum mass of non-rotating configurations (Lasota et al. 1996)

$$M_{\max}^{\text{rot}} \simeq 1.18 M_{\max}^{\text{stat}}. \quad (11.1)$$

However, the above formula is not valid for the EOSs of the form $P/c^2 = a(\rho - \rho_s)$, and in particular, for strange quark stars; their case will be considered in Sect. 12.

In Sect. 8 we derived an absolute upper bound on the static neutron-star mass based on the knowledge of the EOS at $\rho < \rho_u \sim 2\rho_0$ under the constraint of $v_s \leq c$. Let $M_{\max}^{\text{CL,stat}}$ be the upper bound for non-rotating neutron stars. Rotation will increase the upper bound, $M_{\max}^{\text{CL}}(\Omega) > M_{\max}^{\text{CL,stat}}$. The upper bound for rotating stars, $M_{\max}^{\text{CL,rot}}$, is obtained for the same causality-limit EOS as for the non-rotating models; it is reached at Ω very close to Ω_{\max} . Its precise value was obtained by Koranda et al. (1997)

$$v_s \leq c : M_{\max}^{\text{rot}} \leq M_{\max}^{\text{CL,rot}} = 3.89 M_{\odot} \left(\frac{\rho_u}{5 \times 10^{14} \text{ g cm}^{-3}} \right)^{-\frac{1}{2}}. \quad (11.2)$$

For a given ρ_u , it is 30% larger than the static upper bound, $M_{\max}^{\text{CL,stat}}$.

The rapidly rotating configurations, considered in Sects. 10–11, are stable with respect to the axisymmetric perturbations and mass shedding. However, they can be susceptible to various *secular instabilities*, reviewed by Stergioulas (2001).

12 Strange quark stars

By strange stars we will mean the compact objects built entirely, or predominantly, of self-bound strange quark matter (SQM, Sect. 4). The possibility of the existence of self-bound strange quark stars built *entirely* of SQM, was contemplated by Witten (1984), who considered a simplified model of SQM, composed of massless u, d, and s quarks, with the EOS of the form $P = \frac{1}{3}(\rho c^2 - B)$ (see also Brecher and Caporaso 1976). Witten showed that for the bag constant $B \approx 60 \text{ MeV fm}^{-3}$ close to the value needed to reproduce experimental masses of baryons within the MIT Bag Model, the parameters of the maximum-mass configuration for strange stars are similar to those for realistic neutron stars built of baryonic matter. The first detailed models of strange stars, based on a more realistic EOS of SQM, taking into account strange quark mass and the lowest-order QCD interactions, were constructed by Haensel et al. (1986) and Alcock et al. (1986). These authors discussed the basic physical properties of strange stars, and their astrophysical manifestations.

Further development of physics and astrophysics of strange stars focused on the refinement of the EOS of SQM (particularly, beyond the MIT Bag Model), and on specific properties of strange stars, such as neutrino emissivity, rotational properties, superfluidity, pulsations, electromagnetic radiation, and cooling. Physics and astrophysics of strange stars is reviewed by Glendenning (1999), Weber (1999), and Madsen (1999).

The surface density of bare strange stars is equal to that of SQM at zero pressure, ρ_s . It is therefore some fourteen orders of magnitude larger than the surface density of normal neutron stars.

In what follows, we will illustrate the generic properties of strange stars assuming SQM1 EOS of SQM of Zdunik et al. (2001). The $M - R$ curve for bare strange stars is shown in Fig. 9. For strange stars with $M > 1 M_\odot$ the radius changes very little with M , $R \simeq 9 - 11$ km. It is quite similar to that obtained for neutron stars with a moderately stiff EOS. However, at lower masses, the radius of bare strange stars behaves in a completely different way. Namely, it decreases monotonically with decreasing M , and $R \propto M^{\frac{1}{3}}$ for $M \lesssim 0.3 M_\odot$. Such a behavior of low-mass bare strange stars can easily be explained within the bag model. Gravitational pull decreases rapidly with decreasing M , and can be neglected at $M \lesssim 0.3 M_\odot$ compared to the pressure of the normal vacuum on the volume “filled” by the QCD vacuum: this pressure confines SQM to a sphere of radius R . Due to very high incompressibility of strange matter, the density within a low-mass strange star is nearly constant and close to ρ_s (see Fig. 10). On the other hand, the low-mass strange stars can be described in the Newtonian theory, which gives $M \simeq \frac{4\pi}{3} \rho_s R^3$ and $R \propto M^{\frac{1}{3}}$.

The internal structure of bare strange stars is very different from that of neutron stars. First of all, their surface density is huge, $\rho_s \sim 10^{15}$ g cm $^{-3}$. The density profile in such a star is very flat (Fig. 10). Even at the maximum mass, i.e., under the maximum gravitational compression, the central density is only five times higher than the surface one; this is to be compared with fourteen orders of magnitude center-to-surface density difference for neutron stars! The density difference decreases rapidly with decreasing M . For a $1.4 M_\odot$ bare strange star the central density is only forty percent higher than the surface one. For low-mass bare strange stars of $M \lesssim 0.3 M_\odot$, the center-to-surface density difference is negligibly small.

12.1 Maximum mass of strange quark stars

As mentioned before, the EOS of SQM is accurately determined by two parameters, a and ρ_s (Sect. 4). Consider bare strange quark stars. Using the linear representation of the EOS and passing to dimensionless variables \tilde{P} , $\tilde{\rho}$, \tilde{r} ,

$$\tilde{P} = \frac{P}{\rho_s c^2}, \quad \tilde{\rho} = \frac{\rho}{\rho_s}, \quad \tilde{r} = r \cdot \sqrt{\frac{G \rho_s}{c^2}}, \quad (12.1)$$

one can rewrite the equations of hydrostatic equilibrium of strange stars in a dimensionless form. At a fixed a , the equilibrium configuration can be obtained from a universal dimensionless solution of transformed Eqs. (6.1)–(6.2) by returning to ordinary variables r , P , ρ . This property of Eqs. (6.1)–(6.2) implies useful scaling properties relating a solution which corresponds to an EOS $P = a(\rho - \rho'_s)c^2$ to the solution for the EOS $P = a(\rho - \rho_s)c^2$. In particular, the maximum mass for different values ρ_s and ρ'_s are related by the *scaling relation*

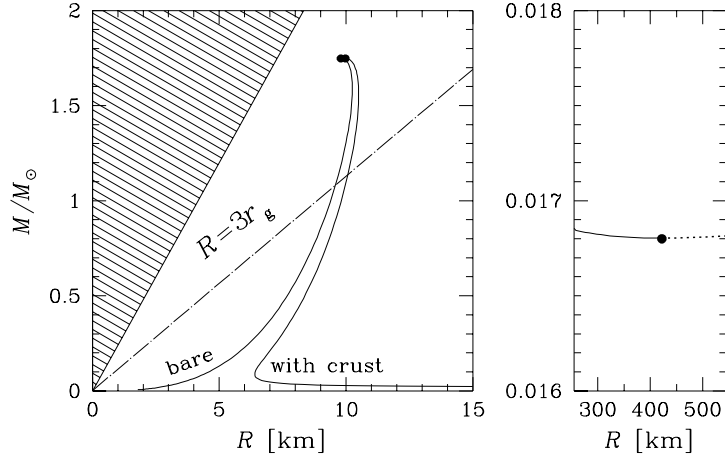


Fig. 9. Mass-radius relation for bare strange stars and for strange stars with normal crust calculated for the SQM1 EOS. Extremal (maximum and minimum mass) configurations are indicated by filled circles. Strange stars with crust have maximum crust mass and thickness: density at the crust bottom is equal to the neutron-drip one, $4.3 \times 10^{11} \text{ g cm}^{-3}$. The dotted segment represents configurations unstable with respect to small radial perturbations. The hatched area corresponds to the region of the $M - R$ plane prohibited by General Relativity and by condition $v_s \leq c$. Long dash-dot line gives the radius of the marginally stable circular orbit around a strange star (it is the radius of the innermost stable orbit of a particle orbiting in the equatorial plane of a non-rotating star). The vicinity of the minimum-mass configuration for strange stars with the crust is shown in the right panel.

$$M'_{\max} = M_{\max} \cdot \left(\frac{\rho_s}{\rho'_s} \right)^{\frac{1}{2}}, \quad (12.2)$$

For a strange matter EOS based on the MIT Bag Model, the scaling relation,

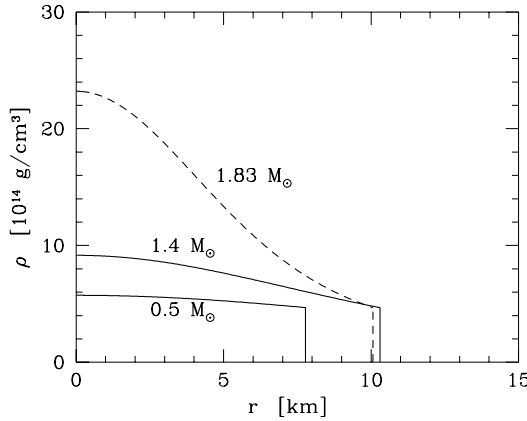


Fig. 10. Mass density ρ versus radial coordinate r for three bare strange stars of different masses, calculated for the SQM1 EOS of strange quark matter. The highest of three masses is the maximum allowable mass for this EOS.

Eq. (12.2), turns out to be precise within better than one percent (Haensel et al. 1986). Similar precision is obtained for other models of SQM (Gondek-Rosińska et al. 2001).

Scaling properties become particularly simple (and actually exact) for the MIT Bag Model EOS with non-interacting massless quarks, i.e., for $a = \frac{1}{3}$ and $\rho_s = 4B/c^2$. This EOS will be referred to as SQM0. The formula for M_{\max} for the SQM0 EOS was derived by Witten (1984),

$$M_{\max} = \frac{1.96}{\sqrt{B_{60}}} M_{\odot} , \quad (12.3)$$

where $B_{60} = B/(60 \text{ MeV fm}^{-3})$.

The scaling formula enables one to explain why the parameters of massive strange stars ($M \sim 1-2 M_{\odot}$) are so similar to what we expect for normal neutron stars. Consider first the simplest SQM0 model. For the hypothesis of strange matter to be correct, energy per unit baryon number in SQM should be less than 930.4 MeV which is the minimum energy per nucleon in normal baryonic matter at zero pressure and temperature; this value is reached for the ^{56}Fe crystal. This condition implies $B_{60} < 1.525$. On the other hand, a consistent model of SQM should not lead to a spontaneous fusion of neutrons into droplets of u, d quarks,

which would eventually transform into droplets of SQM – “strangelets”. This in turn means that the energy per unit baryon number in the u, d matter with $2n_d = n_u$ should be above 939.6 MeV, which implies $B_{60} > 0.982$. All in all, both constraints lead to $1.6 M_\odot < M_{\max} < 2.0 M_\odot$, which reminds us a typical maximum mass range calculated using medium-stiff EOSs of baryon matter. An allowance for the finite mass of the strange quark and for the QCD interactions within the MIT Bag Model can increase maximum masses of strange stars due to a simultaneous decrease of the allowed values of B (this results from the condition $E_{\text{SQM}} < 930.4$ MeV, see Zdunik et al. 2000).

A strange star can be covered by a solid crust of matter with density lower than the neutron drip point (outer neutron-star crust). The nuclei of the crust do not fuse with the SQM core because they are separated from the SQM by a repulsive Coulomb barrier. However, since the mass of the crust is lower than $10^{-4} M_\odot$, its effect on M_{\max} of strange stars is negligible.

12.2 Maximum mass of rotating strange quark stars

Rotation increases the maximum mass of strange quark stars stronger than M_{\max} of neutron stars. This difference results from the different matter distribution within strange quark stars: the density profile is relatively flat and the surface density is huge. This feature increases the effect of centrifugal forces on the stellar structure. For simplest SQM0 EOS one gets the exact result (Gourgoulhon et al. 1999)

$$\text{SQM0 EOS :} \quad M_{\max}^{\text{rot}} = 1.44 M_{\max}^{\text{stat}}. \quad (12.4)$$

In the case of more realistic EOSs of SQM relation (12.4) holds only approximately. Still, one may say that the increase of M_{\max} for strange quark stars due to rapid rotation (about 40%) is twice that for neutron stars (20%).

13 Maximum mass of Q-stars

The models of hypothetical Q-stars were constructed by Bahcall et al. (1990). As mentioned in Sect. 5, two basic parameters of the model are: the energy density U_0 of the scalar field inside the Q-matter and the coupling strength α_v of the vector field to nucleon. The results for Q-star parameters show a simple scaling with U_0 provided the dimensionless parameter $\zeta = \alpha_v U_0^{1/2} \pi / \sqrt{3}$ (Sect. 5) is kept constant. Then, the scaling of M_{\max} with U_0 is the same as that with respect to ρ_s for strange quark stars, Eq. (12.3), but with different numerical coefficients. For $0 \leq \zeta \leq 16$ and $U_0 = 13.0 \text{ MeV/fm}^3$, one gets an astonishingly high maximum allowable mass, $4.0 \leq M_{\max} \leq 8.3 M_\odot$. This stems from a low value of Q-matter density ρ_s at zero pressure: remember that nucleons are nearly massless in the Q-matter. Consider the simplest case of $\zeta = 0$. Then, the EOS for the Q-matter coincides with that for strange matter of massless, non-interacting quarks. However, the standard value used by Bahcall et al. (1990) while constructing the families of the Q-stars is $U_0 = 13.0 \text{ MeV fm}^{-3}$, which corresponds to $\rho_s = 1.0 \times 10^{14} \text{ g cm}^{-3}$, only one

third of the normal nuclear density! The maximum allowable mass can then be calculated using Eq. (12.3), and is $4.0 M_{\odot}$, in agreement with Figs. 4 and 8 of Bahcall et al. (1990). With increasing ζ , the EOS of the Q-matter becomes stiffer. In the limiting case $\zeta = 16$ considered by Bahcall et al. (1990) (at the same value of $U_0 = 13.0 \text{ MeV fm}^{-3}$) they get $\rho_s = 5.5 \times 10^{13} \text{ g cm}^{-3}$ and $M_{\max} = 8.2 M_{\odot}$. This is not surprising: for $a = 1$ ($v_s = c$) we can use a pure-causal limit formula of Sect. 8, getting an estimate of the maximum mass $\approx 9.0 M_{\odot}$. This estimate reproduces within 8% the exact value of M_{\max} , obtained by Bahcall et al. (1990). Rapid rotation could further increase the maximum mass of Q-stars by some 30%, to well above $10 M_{\odot}$.

Summarizing, while the arguments for the existence of Q-matter stem from sophisticated supersymmetric extensions of field-theoretic models of dense nucleon matter, the practical reasons for shockingly high M_{\max} for Q-stars are very simple. Namely, the predicted density of self-bound Q-matter at zero pressure is three to five times lower (!) than the normal nuclear density, which results from a strong reduction of effective nucleon masses in this hypothetical state of matter.

Additional complication is that the typical average density of Q-stars is significantly lower than the nuclear density. Therefore, a conversion of a neutron star into a Q-star should be accompanied by a significant inflation of stellar size, which can be obtained only at the expense of a gigantic work done against the gravitational pull. This should be a very peculiar type of a transformation, in which a compact star becomes less dense, but more bound, because nearly all rest mass of nucleons annihilated in the phase transition. Finally, while the existence of supersymmetric (Q) ground-state of matter may be not in conflict with the terrestrial nuclear physics, reaching this state during stellar evolution may be virtually impossible due to huge energy barrier separating the Q-matter from the normal state of dense matter.

14 Confronting theory with observations

Some neutron stars belong to binary stellar systems. In these cases, one can try to measure their masses by analyzing orbital motion of the binary. Up to now more than one hundred such binary systems containing neutron stars have been discovered which are quite different in nature and observational appearance. In what follows we briefly review evaluations of neutron star masses based on the analysis of binaries containing neutron stars.

The accuracy of measuring masses of X-ray pulsars or X-ray bursters is rather poor because of many obstacles in obtaining high-precision X-ray data, difficulties in establishing the parameters of the orbital motions in the binary and accounting for many interfering factors (e.g., accretion flows, tidal forces). Direct mass estimates have been obtained for several X-ray pulsars and are displayed in Fig. 11. They will be hereafter denoted as M_X .

In what follows, we focus our attention at the binaries with highest M_X . Recent analysis of the mass of neutron star in an X-ray binary, Cyg X-2 (which is an X-ray burster), is – at the 1σ (68%) confidence level $M_X(1\sigma) = 1.78 \pm 0.23 M_{\odot}$.

Simultaneously determined mass of the companion star in Cyg X-2 is $M_c = 0.60 \pm 0.13 M_\odot$ (Orosz and Kuulkers 1999). However, in order to use the value of M_X to constrain dense matter EOS, it seems reasonable to *require* at least 2σ (i.e., 95%) confidence level, which corresponds to $M_X(2\sigma) = 1.78 \pm 0.46 M_\odot$. This would generate $1.32 M_\odot$ as a lower limit on M_{\max} , which is not really useful for constraining modern EOSs of dense matter. With additional constraint on the companion mass, resulting from theoretical models ($M_c > 0.75 M_\odot$), Casares et al. (1998) get $M_X > 1.88 M_\odot$. This would be very restrictive as far as the EOS is concerned, but, in view of additional assumptions and strong model dependence, it cannot be used as a clean measurement of neutron star mass.

Another X-ray binary, studied for a long time, is Vela X-1 (X-ray pulsar). The central value of M_X obtained by different authors is high, $\sim 2 M_\odot$, but the errors are unfortunately quite large. In view of this, the *lower bound* on the mass of Vela X-1 is never significantly higher than $1.4 M_\odot$. Very recently, Barziv et al. (2001) obtained $M_X(2\sigma) > 1.54 M_\odot$ and $M_X(3\sigma) > 1.43 M_\odot$. The 3σ lower bound has (formally) similar significance as the binary – radio-pulsar masses, but is unfortunately close to the mass of the Hulse-Taylor pulsar, and therefore does not yield a new constraint.

Other examples of determination of neutron-star masses of the X-ray pulsars can be found in the paper of van Kerkwijk et al. (1995). One has to conclude, that lower limits on M_{\max} , determined at the 2σ confidence level from the condition $M_{\max} > M_X$, are at present too low to yield useful constraint on the modern dense matter EOS. This situation may change in the future. Very recently, Clark et al. (2002) analysed the high-mass X-ray binary 4U1700-37 (in which the compact star is neither an X-ray pulsar nor an X-ray burster) and found $M_X = 2.44 \pm 0.27 M_\odot$, and $M_X(2\sigma) > 2.0 M_\odot$. If the compact object is a *neutron star* then its mass would rule out soft and moderately stiff EOSs (in particular EOSs which include hyperons and phase transitions).

Observations of kHz quasi-periodic oscillations (QPOs) in low-mass X-ray binaries could (potentially) yield interesting constraints on neutron-star masses in these binary systems, if this phenomenon is connected with the orbital motion of matter around neutron star. However, as by the time of this writing (July 2002), the very mechanism of the phenomenon of the kHz QPOs is not established. Therefore, resulting constraints on neutron-star masses are ambiguous.

Fortunately, there are close binaries containing a radio pulsar and a compact companion (another neutron star or a white dwarf). The presence of a radio pulsar has a great advantage over purely X-ray sources since radio observations enable one to measure the pulsar periods P with extremely high precision (more than 12 correct digits!). Pulsars are known to be excellent timers: their proper rotational periods (in comoving reference frames), in many cases, are wonderfully stable. If, however, a pulsar participates in orbital motion, its period, as measured by a distant observer, varies due to the Doppler effect. Actually, the radio pulses observed on Earth are also influenced by the spacetime curvature in the vicinity of the companion star. Measurable relativistic effects include periastron advance, gravitational redshift and transverse Doppler shift in the orbit, and orbital decay

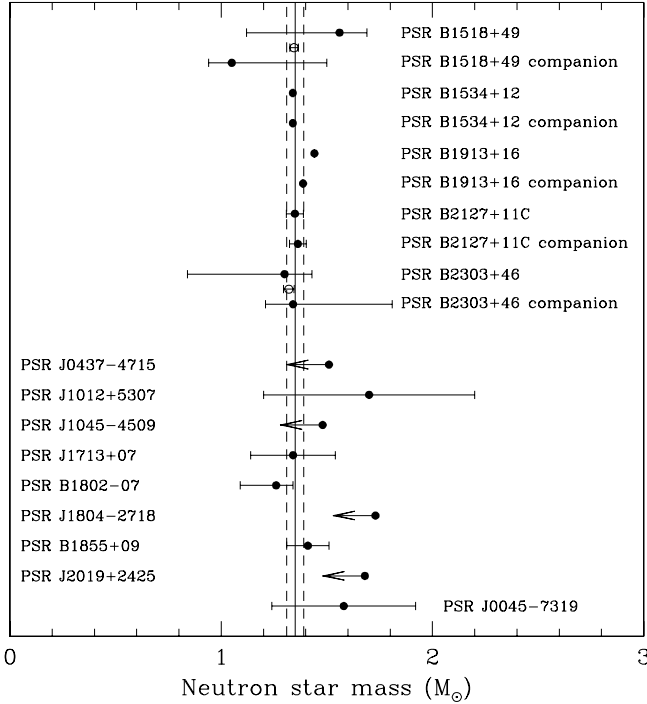


Fig. 11. Neutron star masses from observations of close binaries containing radio pulsars. Error bars indicate 68% (1σ) confidence limits. Upper limits, indicated by arrows, are one-sided 95% (2σ) confidence limits. Estimates of masses of eight neutron stars in four double neutron star systems are shown at the top of the diagram. In two cases, the average neutron star masses in a system is known with much better accuracy than the individual masses; these average masses are indicated with open circles. Estimates of nine neutron stars in neutron star–white dwarf binaries are shown in the central and bottom part of the diagram. The estimate of the neutron-star mass in a neutron star–main-sequence star binary is shown at the bottom of the diagram. Vertical lines are drawn at $M = 1.35 \pm 0.04 M_{\odot}$, and delimit the 68% bounds resulting from the maximum likelihood Gaussian distribution of the measured neutron-star masses, with mean mass $1.35 M_{\odot}$ and standard deviation $0.04 M_{\odot}$. From Thorsett and Chakrabarty (1999).

due to the emission of the gravitational radiation. Under favorable geometrical conditions, Shapiro delay and geodetic precession can also be measured. A review of the present status of the timing analysis of the binary pulsars is given in a *Living Review* by Lorimer (2001).

The masses of six neutron stars in the three neutron-star binaries contain-

ing radio pulsars have been determined with high accuracy. In the case of PSR B1534+12, PSR B1913+16 and their neutron-star companions, the masses are known within 0.2% and 0.02%, respectively. Unfortunately, such double neutron-star systems are expected to be formed in a very specific evolutionary scenario, and therefore the most precisely measured neutron-star masses most probably do not give much information about the complete neutron-star mass function.

An EOS of dense matter has to explain the measured neutron-star masses. A simple rule is to exclude those EOSs which predict lower M_{\max} than the highest *precisely measured* neutron star mass (in July 2002: $1.44 M_{\odot}$; in our opinion result of Clark et al. (2002) has to be carefully checked as far as its model-dependence is concerned before being used to rule out soft and moderately stiff EOSs) At present, this condition excludes only the softest EOSs appearing in literature (some EOSs of dense matter with hyperons: see, e.g., Pandharipande 1971, Balberg and Gal 1997, Vidaña et al. 2000). All of recently developed EOS considered in the present paper are consistent with the Hulse-Taylor pulsar mass (see Fig. 6).

Needless to say, it would be highly desirable to accurately measure the masses of more massive neutron stars, the more massive the better. The highest measured neutron star mass $M_{\text{obs}}^{(\max)}$ implies the observational constraint

$$M_{\max}(\text{EOS}) > M_{\text{obs}}^{(\max)}, \quad (14.1)$$

where $M_{\max}(\text{EOS})$ is maximum allowable mass for static neutron star models for an EOS. Rotation at periods longer than say 5 ms has almost no effect on M_{\max} . A definite discovery of $(1.8 - 2.0) M_{\odot}$ neutron star would rule out EOSs with hyperons and/or phase transitions; the candidates for such massive neutron stars are Vela X-1 and compact star in 4U1700-37, discussed previously in this section. A discovery of, say, $2.1 M_{\odot}$ neutron star would leave us with very stiff EOSs of dense matter containing nucleons only.

15 Concluding remarks

A theorist who strongly believes in the power of the theory could find a loophole in the criterion expressed by Eq. (14.1). Why not imagine two families of “neutron stars”, described by different EOSs which correspond to two different forms (phases) of dense matter. Let the first of them has maximum mass $M_{\max}^{(1)}$ and the second one $M_{\max}^{(2)}$. So one can contemplate a situation, in which the first EOS violates criterion (14.1) but is not eliminated by it because the most massive observed “neutron star” belongs to a second family (Haensel and Zdunik 1989). For example, one might in principle consider the existence of strange quark stars *and* of neutron stars, or even of Q-stars *and* neutron stars. Of course, a necessary condition for some contact with reality is the stability of *both* these families. This means, that at the same baryon numbers compact star configurations belonging to different families have to be separated by a sufficiently high energy barrier.

How far can one go with theoretical considerations not substantiated by solid experimental basis? Many theorists (to which the author belongs) think that re-

specting the *Occam's razor* principle is necessary in research work.⁸ The fact that a model is not ruled out by observations is not a proof of its reality. The model has to be *necessary* for understanding the observations to be considered as representing a reality. It would be intellectually arrogant to believe that the universe is filled with objects predicted by the theories based on a distant extrapolation of the laboratory physics. Conventional models of neutron stars should be considered as long as they are sufficient to understand astrophysical phenomena and measurements. If one day a compact object of, say, $8 M_{\odot}$ is discovered which is not a black hole, then it cannot be but a Q-star. Future observations will hopefully bring us more information, and enrich our knowledge of the compact stars, but for the time being the principle devised by William of Occam is a useful complement to the theory of dense matter.

Acknowledgements. The author is deeply grateful to D.G. Yakovlev for reading the manuscript and for helpful remarks and comments. He is also very grateful to A.Y. Potekhin for his precious help in the preparation of figures. This work was supported by the KBN grant No. 5 P03D 020 20.

References

Akmal, A., Pandharipande, V.R., Ravenhall, D.G., 1998, *Phys. Rev. C* **58**, 1804
 Alcock, C., Farhi, E., Olinto, A.V., 1986, *Astrophys. J.* **310**, 261
 Backer, D.C., Kulkarni, S.R., Heiles, C., et al., 1982, *Nature* **300**, 615
 Bahcall, S., Lynn, B.W., Selipsky, S.B., 1990, *Astrophys. J.* **362**, 251
 Balberg, S., Gal, A., 1997, *Nucl. Phys. A* **625**, 435
 Baldo, M., Bombaci, I., Burgio, G.F., 1997, *Astron. Astrophys.* **328**, 274
 Barziv, O., Kaper, L., Van Kerkwijk, M.H., et al., *Astron. Astrophys.* **377**, 925
 Baumgarte, T.W., Shapiro, S.L., Teukolsky, S.A., 1996a, *Astrophys. J.* **458**, 680
 Baumgarte, T.W., Janka, H.-T., Keil, W., Shapiro, S.L., Teukolsky, S.A., 1996b, *Astrophys. J.* **468**, 823
 Baym, G., Pethick, C.J., Sutherland, P., 1971, *Astrophys. J.* **170**, 299
 Bombaci, I., 1995, in *Perspectives on Theoretical Nuclear Physics*, ed. I. Bombaci, A. Bonnaccorso, A. Fabrocini, et al., 223
 Brecher, K., Caporaso, C., 1976, *Nature* **259**, 377
 Brown, G.E., Weise, W., 1976, *Phys. Rep.* **27**, 1
 Casares, J., Charles, P., Kuulkers, E., 1998, *Astrophys. J.* **493**, L39
 Chanmugam, G., 1977, *Astrophys. J.* **217**, 799
 Chanmugam, G., Gabriel, M., 1971, *Astron. Astrophys.* **13**, 374
 Clark, J.S., Goodwin, S.P., Crowther, P.A., 2002, *Astron. Astrophys.* **392**, 909
 Cook, G.B., Shapiro, S.L., Teukolsky, S.A., 1994, *Astrophys. J.* **424**, 823

⁸Occam's razor: a principle stating that entities must not be multiplied beyond what is necessary; often interpreted to mean that phenomena should be explained in terms of the simplest possible causes. William of Occam was a medieval English philosopher who devised this principle.

Dey, M., Bombaci, I., Dey, J., Ray, S., Samanta, B.C., 1998, *Phys. Lett. B* **438**, 123

Douchin, F., Haensel, P., 2001, *Phys. Lett. B* **485**, 107

Douchin, F., Haensel, P., 2001, *Astron. Astrophys. B* **380**, 151

Drago, A., Tambini, U., Hjorth-Jensen, M., 1996, *Phys. Lett. B* **380**, 13

Farhi, E., Jaffe, R.L., 1984, *Phys. Rev. D* **30**, 2379

Glendenning, N.K., 1999, Compact stars: nuclear physics, particle physics, and general relativity, (second edition), Springer, New York

Glendenning, N.K., Kettner, C., 2000, *Astron. Astrophys. 353*, L9

Gondek-Rosińska, D., Bulik, T., Zdunik, L., et al., 2000, *Astron. Astrophys. 363*, 1005

Gourgoulhon, E., Haensel, P., 1993, *Astron. Astrophys. 271*, 187

Gourgoulhon, E., Haensel, P., Gondek, D., 1995, *Astron. Astrophys. 294*, 747

Gourgoulhon, E., Haensel, P., Livine, R., Paluch, E., Bonazzola, S., Marck, J.-A., 1999, *Astron. Astrophys. 349*, 851

Haensel, P., Prószyński, M., 1982, *Astrophys. J. 258*, 306

Haensel, P., Zdunik, J.L., Schaeffer, R., 1986, *Astron. Astrophys. 160*, 121

Haensel, P., Zdunik, 1989, *Nature 340*, 317

Haensel, P., Zdunik, J.L., 1990, *Astron. Astrophys. 229*, 117

Haensel, P., Pichon, B., 1994, *Astron. Astrophys. 283*, 313

Haensel, P., Zdunik, J.L., Douchin, F., 2002, *Astron. Astrophys. 385*, 301

Harrison, B.K., Thorne, K.S., Wakano, M., Wheeler, J.A., 1965, Gravitation theory and gravitational collapse, University of Chicago Press, Chicago

Hartle, J.B., Sawyer, R.F., Scalapino, D.J., 1975, *Astrophys. J. 199*, 471

Hartle, J.B., 1978, *Phys. Reports 46*, 201

Kaempfer, B., 1981, *Phys. Lett. 101 B*, 366

Kaempfer, B., 1982, *Astron. Nachr. 303*, 231

Kalogera, V., Baym, G., 1996, *Astrophys. J. 470*, L61

Koranda, S., Stergioulas, N., Friedman, J.L., 1997, *Astrophys. J. 488*, 799

Kusenko, A., Shaposhnikov, M., Tinyakov, P.G., Tkachev, I.I., 1998, *Phys. Lett. B* **423**, 104

Kusenko, A., 2000, in Dark Matter in Astro- and Particle Physics (Dark 2000), p. 306-315, [hep-ph/0009089](#)

Landau, L.D., 1932, *Phys. Z. Sowjetunion*, **1**, 285 (reprinted in: Gursky, H., Ruffini, R., 1975, Neutron Stars, Black Holes, and Binary X-ray Sources, Reidel, Dordrecht, p. 271)

Landau, L.D., Lifshitz, E.M., 1980, Fluid Mechanics, Pergamon Press, Oxford

Landau, L.D., Lifshitz, E.M., 1999, The Classical Theory of Fields, Butterworth-Heinemann, Oxford

Lasota, J.-P., Haensel, P., Abramowicz, M.A., 1996, *Astrophys. J.* **456**, 300

Lee, T.D., Wick, G.C., 1974, *Phys. Rev. D* **9**, 2291

Lee, T.D., 1975, *Rev. Mod. Phys.* **47**, 267

Lighthill, M.J., 1950, *Month. Not. Roy. Astron. Soc.* **110**, 337

Lorenz, C.P., 1991, Ph.D. Thesis, University of Illinois, Urbana-Champaign

Lorenz, C.P., Ravenhall, D.G., Pethick, C.J., 1993, *Phys. Rev. Lett.* **70**, 379

Lorimer, D.R., 2001, Binary and Millisecond Pulsars in the New Millennium, *Living Rev. Relativity* **4** (2001) 5. [Online Article]: cited on 11 December 2001, <http://www.livingreviews.org/Articles/Volume4/2001-5lorimer/>

Lyne, A.G., Graham-Smith, F., 1998, Pulsar astronomy, 2nd edition, Cambridge University Press, Cambridge

Madsen, J., 1999, in Hadrons in dense matter and hadrosynthesis, Cleymans, J., ed., Lecture Notes in Physics, Springer-Verlag, p. 162

Meltzner, D.W., Thorne, K.S., 1966, *Astrophys. J.* **145**, 514

Migdal, A.B., 1971, *Zh. Exp. Teoret. Fiz.* **61**, 1184

Migdal, A.B., 1972, *Soviet Phys. - JETP* **36**, 1052

Migdal, A.S.B., 1973, *Phys. Rev. Lett.* **31**, 257

Migdal, A.B., 1974, *Phys. Lett.* **52 B**, 172

Migdal, A.B., Saperstein, E.E., Troitsky, M.A., Voskresensky, D.N., 1990, *Phys. Repts.* **192**, 179

Misner, C.W., Thorne, K.S., Wheeler, J.A., 1973, Gravitation, W.H. Freeman and Co., San Francisco

Moszkowski, S.A., Källman, C.-G., 1977, *Nucl. Phys. A* **287**, 495

Oppenheimer, J.R., G.M. Volkoff, G.M., 1939, *Phys. Rev.* **55**, 374

Orosz, J.A., Kuulkers, E., 1999, *MNRAS* **305**, 1320

Pandharipande, 1971, V.R., *Nucl. Phys. A* **178**, 123

Pandharipande, V.R., Smith, R.A., 1975, *Phys. Lett.* **59 B**, 15

Pandharipande, V.R., Ravenhall, D.G., 1989, in Proc. NATO Advanced Research Workshop on nuclear and heavy ion collisions, Les Houches 1989, ed. M. Soyeur et al., Plenum, New York, p. 103

Rhoades, C.J., Jr., Ruffini, R., 1974, *Phys. Rev. Letters* **32**, 324

Ramsey, W.H., 1950, *Monthly Not. Roy. Astron. Soc.* **110**, 325

Schaeffner-Bielich, J., Hanauske, M., Stöcker, H., Greiner, W., 2002, *Phys. Rev. Lett.* **89**, 171101

Seidov, Z.F., 1971, *Soviet Astronomy - Astron. Zh.* **15**, 347

Shapiro, S.L., Teukolsky, S.A., 1983, Black Holes, White Dwarfs, and Neutron Stars, Wiley, New York

Stergioulas, N., 2001, Rotating Stars in Relativity, *Living Rev. Relativity* **1** (1998) 8. [Online Article]: cited on 11 December 2001, <http://www.livingreviews.org/Articles/Volume1/1998-8stergio/>

Sumiyoshi, K., Yamada, S., Suzuki, H., Hillebrandt, W., 1998, *Astron. Astrophys.* **334**, 159

Vidana, I., Polls, A., Ramos, A., Engvik, L., Hjorth-Jensen, M., 2000, *Phys. Rev. C* **62**, 035801

Weber, F., 1999, Pulsars as astrophysical laboratories for nuclear and particle physics, IoP Publishing, Bristol and Philadelphia

Weinberg, S., 1972, Gravitation and cosmology: principles and applications of the general theory of relativity, John Wiley and Sons, New York

Wiringa, R.B., Fiks, V., Fabrocini, A., 1988, *Phys. Rev. C* **38**, 1010

Witten, E., 1984, *Phys. Rev. C* **30**, 272

Zdunik, J.L., P.Haensel, P., Schaeffer, R., 1987, *Astron. Astrophys.* **172**, 95

Zdunik, J.L., 2000, *Astron. Astrophys.* **359**, 311

Zdunik, J.L., Bulik, T., Kluźniak, W., Haensel, P., Gondek-Rosińska, D., 2000, *Astron. Astrophys.* **359**, 143

Zdunik, J.L., Haensel, P., Gourgoulhon, E., 2001, *Astron. Astrophys.* **372**, 535

Zeldovich, Ya.B., 1962, *Sov. Phys. - JETP* **14**, 1143

Zeldovich, Ya.B., Novikov, I.D., 1971, Relativistic astrophysics, vol. 1, University of Chicago Press, Chicago